Original Article

JCBFM

Journal of Cerebral Blood Flow & Metabolism
2017, Vol. 37(4) 1299–1310

DOI: 10.1177/0271678X16654494
journals.sagepub.com/home/jcbfm
SAGE

Low-density lipoprotein receptor-related protein-1 facilitates heme scavenging after intracerebral hemorrhage in mice

Gaiqing Wang[1,2], Anatol Manaenko[1], Anwen Shao[1], Yibo Ou[1], Peng Yang[1], Enkhjargal Budbazar[1], Derek Nowrangi[1], John H Zhang[1,3] and Jiping Tang[1]

Abstract

Heme-degradation after erythrocyte lysis plays an important role in the pathophysiology of intracerebral hemorrhage. Low-density lipoprotein receptor-related protein-1 is a receptor expressed predominately at the neurovascular interface, which facilitates the clearance of the hemopexin and heme complex. In the present study, we investigated the role of low-density lipoprotein receptor-related protein-1 in heme removal and neuroprotection in a mouse model of intracerebral hemorrhage. Endogenous low-density lipoprotein receptor-related protein-1 and hemopexin were increased in ipsilateral brain after intracerebral hemorrhage, accompanied by increased hemoglobin levels, brain water content, blood–brain barrier permeability and neurological deficits. Exogenous human recombinant low-density lipoprotein receptor-related protein-1 protein reduced hematoma volume, brain water content surrounding hematoma, blood–brain barrier permeability and improved neurological function three days after intracerebral hemorrhage. The expression of malondialdehyde, fluoro-Jade C positive cells and cleaved caspase 3 was increased three days after intracerebral hemorrhage in the ipsilateral brain tissues and decreased with recombinant low-density lipoprotein receptor-related protein-1. Intracerebral hemorrhage decreased and recombinant low-density lipoprotein receptor-related protein-1 increased the levels of superoxide dismutase 1. Low-density lipoprotein receptor-related protein-1 siRNA reduced the effect of human recombinant low-density lipoprotein receptor-related protein-1 on all outcomes measured. Collectively, our findings suggest that low-density lipoprotein receptor-related protein-1 contributed to heme clearance and blood–brain barrier protection after intracerebral hemorrhage. The use of low-density lipoprotein receptor-related protein-1 as supplement provides a novel approach to ameliorating intracerebral hemorrhage brain injury via its pleiotropic neuroprotective effects.

Keywords

Intracerebral hemorrhage, blood–brain barrier permeability, brain edema, heme scavenging, low-density lipoprotein receptor-related protein-1

Received 1 February 2016; Revised 14 April 2016; Accepted 10 May 2016

Introduction

Intracerebral hemorrhage (ICH) is the most common type of hemorrhagic stroke and has the highest mortality rate of all stroke subtypes.[1,2] The rapid accumulation of blood within the brain parenchyma leads to the disruption of the normal anatomy and results in an increase of local pressure.[3] Following the initial ictus, the resulting hematoma triggers a series of secondary brain injury events. The extravasated blood and its components trigger the formation of brain swelling, tissue death, and impose a strong cytotoxic,

[1]Department of Physiology, Loma Linda University, Loma Linda, CA, USA
[2]Department of Neurology, The Second Hospital, Shanxi Medical University, Taiyuan, Shanxi, China
[3]Department of Anesthesiology, Loma Linda University, Loma Linda, CA, USA

Corresponding author:
Jiping Tang, Department of Physiology, Loma Linda University School of Medicine, Loma Linda, CA 92354, USA.
Email: jtang@llu.edu

pro-oxidative, and proinflammatory insult to the adjacent tissue which can be observed within minutes after the initial ICH event.[3,4] These conditions can result in damage to surrounding neuronal tissue and the blood–brain barrier (BBB), thus increasing edema formation and decreasing neurological functions.

Blood plasma components present in the brain tissue early after the ICH injury include blood-derived coagulation factors, complement components, immunoglobulins, and other bioactive molecules considered to be toxic substances that generate tissue damage.[3,5,7] Hemoglobin (Hb) and its degradation products, heme and iron, are potent cytotoxic components that can induce cell death and disrupt the BBB.[8] The prominent mechanism of Hb toxicity is via the generation of free radicals (mainly through a Fenton-type mechanism) and the resulting oxidative damage to proteins, nucleic acids, carbohydrates, and lipids.[2,4,9,10] The removal of the hematoma and its blood components may be a key strategy to ameliorating the brain injury and improving recovery following ICH.

Low-density lipoprotein receptor-related protein-1 (LRP1) is a transmembrane receptor expressed on several cells types including macrophages, hepatocytes, neurons, vascular endothelial cells, pericytes, smooth muscle cells, and astrocytes.[11,13]

The receptor has been identified to have a multifunctional role as a cargo transporter, signaling receptor for lipid endocytosis, and protein scavenging.[14,15] A key function defined for LRP1 has been its integral role with inducing systemic heme clearance. Free heme is highly toxic due to its oxidative and proinflammatory effects. LRP1 has been identified as a receptor for free heme, hemopexin (Hx), and the Hx–heme complex. Hx is a high-affinity heme scavenging protein found prominently in plasma and cerebrospinal fluid that binds with heme to form the Hx–heme complex. The formation of the Hx–heme complex facilitates the cellular metabolism of heme, also decreasing available free heme levels, thus preventing its cytotoxic effects.[16]

LRP1 have been recently identified as a primary receptor responsible for uptake of Hx–heme complexes in humans.[17] Upon binding of heme–Hx to LRP1, the complex becomes internalized via endocytosis into cells. Inside the cell, the heme–Hx complex is dissociated by lysosomal activity. Heme is catabolized by heme oxygenases into biliverdin, carbon monoxide, and iron.[18,19] LRP1 is upregulated in neurons and astrocytes as a response to increased iron concentration[20] and its expression correlated with iron status.[21] There are indications that the activation of LRP1 scavenging system in humans has favorable effects after subarachnoid hemorrhage (SAH).[22] Effects of the activation of LRP1 system after ICH have not been evaluated yet and the findings, as mentioned above, let us hypothesize that the activation of the LRP1 system will have beneficial, clinically translatable effects after ICH.

In this study, we suggest that elevating LRP1 activity will increase Hx–heme clearance, therefore reducing cytotoxic cell death and improving BBB integrity after ICH in a collagenase infusion model in mice.

Materials and methods

Animals

Eight-week-old male CD1 mice (weight $30\,g \pm 5\,g$; Charles River, Wilmington, MA) were housed in a vivarium for a minimum of three days before surgery with a 12 h light/dark cycle and ad libitum access to food and water. All procedures in this study were approved by the Institutional Animal Care and Use Committee at Loma Linda University and comply with the National Institutes of Health's Guide for the Care and Use of Laboratory Animals, and the manuscript adheres to the ARRIVE (Animal Research: Reporting of In Vivo Experiments) guidelines for reporting animal experiments.

Experimental design

The experiments were performed in a mouse model of ICH. A total of 134 mice were used. Animals were randomly divided into different experimental groups. Animals, which died before final assessment, were replaced. There were no significant differences in the mortality rate between the different experimental groups.

Seventeen animals are designated for sham, 22 for ICH by collagenase (i.c.), 19 for ICH + vehicle (saline, ntracerebroventricular (i.c.v).), 18 for ICH + human LRP1 recombinant protein (50 ng, i.c.v.), 19 for ICH + control siRNA (control siRNA, i.c.v.), 19 for ICH + LRP1 (100 pmol LRP1 siRNA, i.c.v.), and 20 for ICH + LRP1 siRNA + human LRP1 recombinant protein (100 pmol LRP1 siRNA, i.c.v.; 50 ng r-LRP1, i.c.v.) were used.

Experiment 1 was to characterize the time course of endogenous changes in LRP1 and Hx levels in ipsilateral/right hemisphere at 1, 3, 7, and 14 days after ICH. Twenty-seven mice were randomized into five groups: sham, ICH-1d, ICH-3d, ICH-7d and ICH-14d ($n = 5$/group). Two mice in ICH group died during surgery, one on days 1 and 2 each.

Experiment 2 was to evaluate the role of LRP1 in the pathophysiology of ICH. First, we tested the effect of the exogenous LRP1 (recombinant human LRP1 protein; r-LRP1). Fifty-seven mice were used in the following groups: sham ($n = 17$), ICH + vehicle ($n = 19$), ICH + r-LRP1 ($n = 18$). r-LRP1 recombinant protein

(50 ng in 1 μl saline; MyBioSource) was administered by i.c.v injection 20 min before the induction of ICH. The vehicle group was treated with the same volume of saline. Second, we investigated whether inhibition of LRP1 (LRP1 siRNA) mediates the repression of LRP1-Hx signaling. Thirty mice in two additional groups were added: ICH + control siRNA (n = 19) and ICH + LRP1 siRNA (n = 19). The 100 pmol of LRP1 siRNA (mouse, Santa Cruz Biotechnology) was dissolved in 1 μl of sterilized RNase free water and injected intracerebroventricularly 24 h before ICH.[23] The same volume of control siRNA (negative controls, Santa Cruz Biotechnology) was administered as a control. Third, we tested the effects of LRP1 using siRNA-mediated LRP1 gene silencer and r-LRP1 protein. An additional group of ICH + LRP1 siRNA + r-LRP1 (n = 20) was added.

ICH surgery

Experimental ICH was induced by intrastriatal injection of collagenase (0.075 units in 0.5 μl saline, VII-S; Sigma, St Louis, MO, USA) into the basal ganglia as we have previously described.[24] Briefly, mice were anesthetized with an intraperitoneal injection of ketamine (100 mg/kg) and xylazine (10 mg/kg) and positioned prone in a stereotaxic head frame (Stoelting, Wood Dale, IL, USA). An electronic thermostat-controlled warming blanket was used to maintain the core temperature at 37°C. A cranial burr hole (1 mm) was drilled and a 26-gauge needle on a 10 μl Hamilton syringe was inserted stereotactically into the right basal ganglia (coordinates: 0.9 mm posterior to the bregma, 1.5 mm lateral to the midline, and 4 mm below the dura mater). The collagenase was infused at a rate of 0.25 μl/min over 2 min with an infusion pump (Stoelting, Harvard Apparatus, USA). The needle was left in place for an additional 10 min after injection to prevent possible leakage of the collagenase solution. After removal of the needle, the burr hole was closed using bone wax, the incision was sutured, and the mice were allowed to recover. Sham-operated mice were subjected to needle insertion only. Vital signs were monitored throughout surgery and recovery. At every time point (6 h, 1, 3, 7, and 14 days) after surgery, neurological functions were assessed. Following neurofunctional testing, the animals were euthanized for measurements of brain water content, hematoma volume, BBB permeability (Evans blue assay), Western blot, and immunohistochemistry assay as described below.

Intracerebroventricular injection

According to the manufacturer's instructions, 100 pmol of control or LRP1 siRNA or 50 ng r-LRP1[23] was dissolved in 1 μl of sterile 0.9% saline and stereotactically injected into the right lateral ventricle at a rate of 0.25 μl/min (coordinates: 0 mm bregma, 1 mm lateral, and 3.5 mm ventral) using a 26-gauge needle. The control and LRP1 siRNA were administered 24 h before the induction of ICH and r-LRP1 30 min before ICH.

Neurobehavior exams

Neurobehavior tests were assessed at 24 and 72 h after the ICH surgery by an independent researcher blinded to the procedure. Three tests were implemented to evaluate neurological deficits: (1) modified Garcia test, (2) wire hang, and (3) beam balance. The modified Garcia exam was composed of seven subtests which were each scored out of three points (total = 21 points). The test included were (i) spontaneous activity, (ii) response to vibrissae touch, (iii) body proprioception, (iv) symmetry in the movement of four limbs, (v) forepaw outstretching, (vi) lateral turning, and (vii) climbing. Higher scores indicate greater neurofunction (healthy mouse).

Wire hanging and beam balance tests were performed as previously described.[23] Bridges between platforms were built with wire (length, 50 cm; diameter, 1 mm) and beam (length, 90 cm; diameter, 1 cm). Mice were put on the center of the wire or beam and allowed to reach the platform. Mice were observed for both their time and behavior until they reached one platform and scored according to six grades. The test was repeated three times, and an average score was taken (minimum score = 0; maximum score (healthy mouse) = 5). All behavioral tests were conducted by the investigator, blinded to the experiment groups.

Brain water content

The brain water content and neurological deficits were evaluated as previously described using the wet/dry method.[25] Briefly, mice were euthanized under deep anesthesia. Brains were removed immediately and divided into five parts: ipsilateral and contralateral basal ganglia, ipsilateral and contralateral cortex, and cerebellum. The cerebellum was used as an internal control for brain water content. Tissue samples were weighed on an electronic analytical balance (APX-60, Denver Instrument) to the nearest 0.1 mg to obtain the wet weight. The tissue was then dried at 100°C for 48 h to determine the dry weight. Brain water content (%) was calculated as ((wet weight − dry weight)/wet weight) × 100.

Evans blue extravasation

BBB permeability using Evans blue extravasation was evaluated as previously described.[26] A 2% solution of

Evans blue dye in normal saline (4 ml/kg of body weight) was injected into the jugular vein. After allowing it to circulate for 1 h, the mice were transcardially perfused with 100 ml of ice-cold phosphate-buffered saline (PBS). The brain tissue was removed and divided into right and left hemispheres, frozen in liquid nitrogen, and stored at −80°C until analysis. The samples were homogenized in 1100 µl of PBS, sonicated, and centrifuged (30 min, 15,000 r/min, 4°C). The supernatant was collected and for each 500 µl sample an equal amount of 50% trichloroacetic acid was added. The samples were incubated over night at 4°C and then centrifuged (30 min, 15,000 r/min, 4°C). Evans blue stain was measured by spectrophotometer (Thermo Scientific™ GENESYS 10 S UV-Vis spectrophotometer, USA) at 610 nm and quantified according to a standard curve. These data were calculated as µg of Evans blue dye/g of tissue and represented as a ratio compared to sham.

Hemoglobin assay

For hematoma evaluation, supernatant collection was completed using the same method as the Evans blue extravasation. Following the supernatant collection, Drabkin's reagent (0.4 ml, Sigma-Aldrich) was added to 0.1 ml supernatant aliquots and allowed to rest for 15 min at room temperature, protected from light. Optical density was measured and recorded at 540 nm with a spectrophotometer (Thermo Scientific™ GENESYS 10S UV-Vis spectrophotometer, USA). These procedures yielded a linear relationship between measured hemoglobin concentrations in perfused brain and the volume of added blood on a standard curve.

Western blot

Western Blot was performed for proteins as previously described.[23,25] Briefly, the right cerebral hemispheres were homogenized, and protein concentration was acquired for each sample using a detergent compatible assay (Bio-Rad, Philadelphia, PA). Protein samples (50 µg) were loaded on a tris-glycine gel, electrophoresed, and transferred to a nitrocellulose membrane. Membranes were incubated overnight at 4°C with the primary antibodies: rabbit polyclonal anti-LRP1 (1:300,000 abcam), rabbit polyclonal anti-Hx (1:2000 abcam), rabbit polyclonal anti-malondialdehyde (MDA, 1:5000 abcam), rabbit polyclonal anti-superoxide dismutase 1 (SOD1, 1:2000 Santa Cruz Bio) and rabbit polyclonal anti-caspase 3 (1:1000 cell signaling). The same membrane was probed with an antibody against β-actin (Santa Cruz, 1:5000) as an internal control after being stripped. Incubation with secondary antibodies (Santa Cruz Biotech) was done for 1 h at room temperature. Immunoblots were then probed with an ECL Plus chemiluminescence reagent kit (Amersham Biosciences, Arlington Heights, IL) and visualized with an imaging system (Bio-Rad, Versa Doc, model 4000). Data were analyzed using Image J software.

Immunohistochemistry

Immunohistochemistry was performed as described previously.[27] The brains were cut into 10 µm thick coronal sections in a cryostat (CM3050S; Leica Microsystems). The sections were incubated overnight at 4°C with the following primary antibodies: rabbit anti-LRP1 (1:100), goat anti-ionized calcium-binding adaptor molecule 1 (Iba1, 1:100, Abcam), goat anti-Glial fibrillary acidic protein (GFAP, 1:100, Santa Cruz), goat polyclonal anti-Von Willebrand Factor (vWF, 1:100, Abcam), and rabbit anti-Hx (1:100) followed by incubation with appropriate FITC-conjugated or Alexa Fluor-conjugated secondary antibodies (Jackson Immuno Research). Negative control staining was performed by omitting the primary antibody. Perihemorrhagic area of the brain coronal sections was visualized with a fluorescence microscope (Olympus BX51).

Fluoro-Jade C (FJC) staining (Biosensis) was used to identify irreversibly degenerating neurons.[28] Following manufacturer's protocol, the sections were rinsed in basic alcohol for 5 min followed by a 2 min rinse in 70% alcohol. The sections were then briefly rinsed in distilled water and incubated in 0.06% potassium permanganate for 10 min, and then briefly rinsed in distilled water to remove excess potassium permanganate. Samples were then incubated in 0.0001% FJC stain in 0.1% acetic acid for 10 min. Following FJC labeling, the sections were rinsed three times in distilled water for 5 min each, air dried for 10 min, cleared in xylene, and covered with DPX.

Statistics

Quantitative data are presented as mean ± SD. One-way ANOVA for multiple comparisons with Tukey's post-hoc test were used to determine the differences of brain water content, neurological deficits, and Western blot assay among all groups at each time point. A $p < 0.05$ was considered statistically significant.

Results

Mortality

All sham-operated mice survived. The total operative mortality of mice was about 9% (n = 12). The mortality

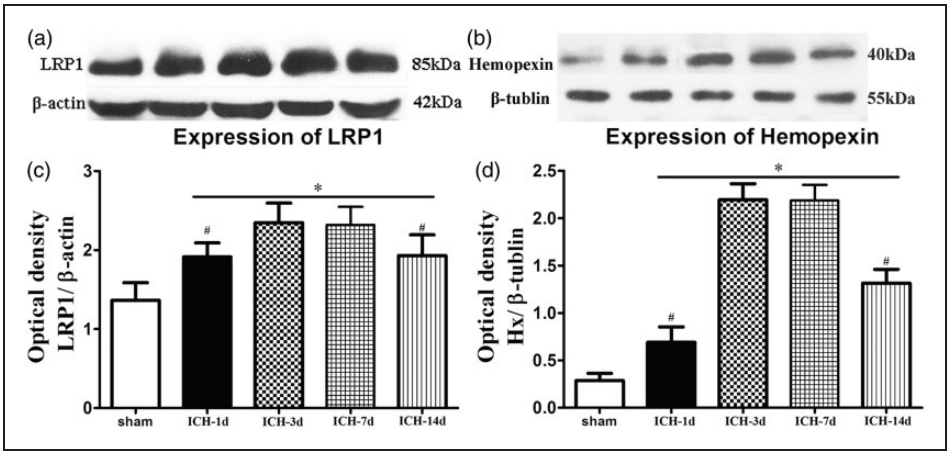

Figure 1. Time course in protein levels of LRP1 and hemopexin changes within ipsilateral brain tissues after ICH (a and b). Quantitative analysis with Western blot shows that LRP1 and hemopexin levels increased at 1, 3, 7 days and 14 days after ICH (c and d; n = 5/group). One-way ANOVA followed by Tukey's test were used.*$p < 0.05$ versus sham; #$p < 0.05$ versus ICH-3d.

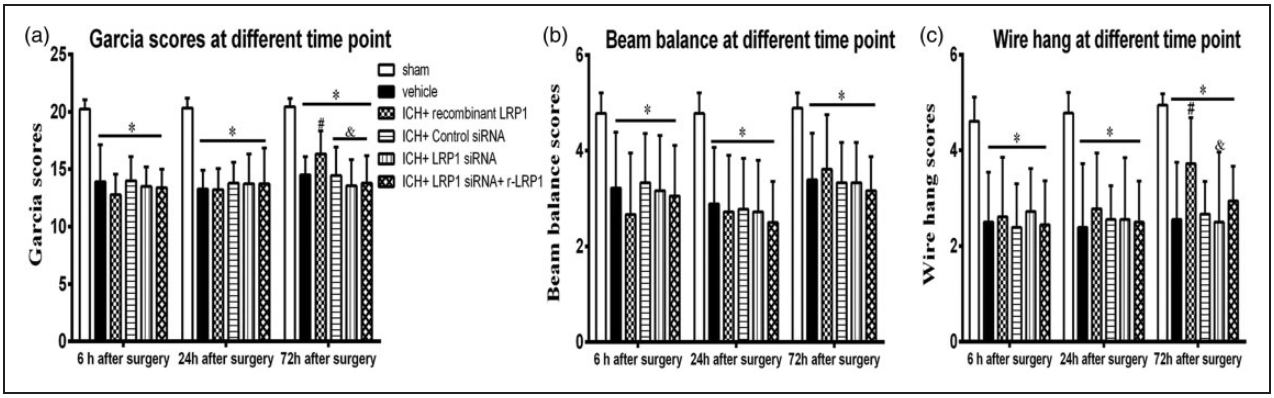

Figure 2. Effect of LRP1 on modified Garcia test, balance beam test and wire hang test 6, 24 and 72 h after ICH (a to c). (n = 18/group). One-way ANOVA followed by Tukey tests were used. *$p < 0.05$ versus sham; #$p < 0.05$ versus vehicle; &$p < 0.05$ versus human recombinant LRP1-treated ICH.

was not significantly different among the experimental groups (data not shown).

Endogenous LRP1 and Hx expression increased after ICH

Western blot showed a significant increase in LRP1 and Hx protein expression within ipsilateral brain tissues at 1, 3, 7 and 14 days after ICH compared to sham ($p < 0.05$, Figure 1(a) and (b)). The expression levels reached a maximum at three to seven days following ICH.

r-LRP1 improved neurobehavior following ICH

ICH + vehicle animals scored significantly lower compared to sham mice in all neurobehavior tests performed at each time point ($p < 0.05$, Figure 2(a) to (c)). In all neurobehavior tests, all groups were significant to sham at 6, 24, and 72 h after ICH ($p < 0.05$). However, compared with ICH + vehicle, r-LRP1 showed significant improvement in the modified Garcia test and the wire Hang 72 h after ICH ($p < 0.05$, Figure 2(a) and (c)) but not in the beam balance test ($p > 0.05$, Figure 2(b)) (n = 18/group). LRP1 siRNA countered the beneficial effect of the r-LRP1 on neurological outcome and did not reach significance against ICH + vehicle at three days after ICH ($p > 0.05$, Figure 2(a) and (c)). Following these results, we choose to examine the mechanism of LRP1 three days after ICH for future studies.

r-LRP1 decreases hematoma volume, BBB permeability, and brain water content three days following ICH

All groups showed a significant increase in hemoglobin levels, Evans blue extravasation, and brain water

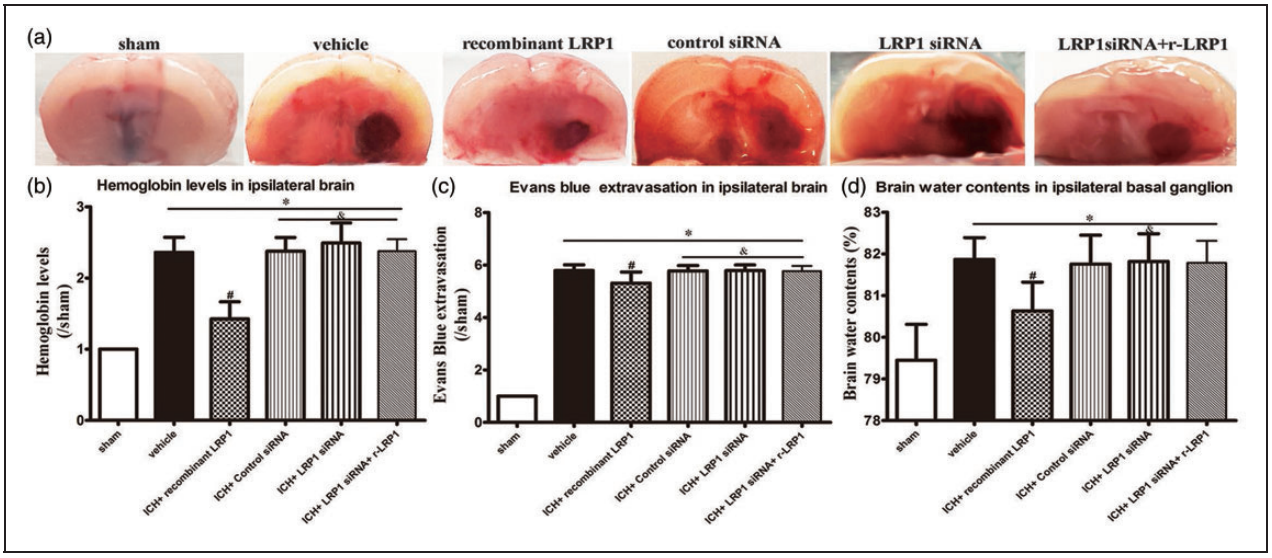

Figure 3. Effect of LRP1 on hematoma volume, blood–brain barrier permeability and brain water content 72 h after ICH (a to d). One-way ANOVA followed by Tukey tests were used. *$p < 0.05$ versus sham; #$p < 0.05$ versus vehicle; &$p < 0.05$ versus human recombinant LRP1-treated ICH.

content compared with sham ($p < 0.05$, Figure 3(a) to (d)). r-LRP1 significantly reduced hematoma volume, brain water content and BBB permeability compared with the ICH + vehicle group ($p < 0.05$, Figure 3(a) to (d)). LRP1 siRNA and control siRNA countered the beneficial effect of the r-LRP1on ICH ($p > 0.05$). r-LRP1 was not able to reverse the effects of LRP1 siRNA and did not reach significance against vehicle ($p > 0.05$, Figure 3(a) to (d)).

r-LRP1 increases Hx–heme scavenging three days after ICH

Western blot analysis was done on LRP1 and Hx on ipsilateral brain tissue. LRP1 was significantly elevated in ICH + vehicle, ICH + r-LRP1, and ICH + control siRNA groups compared to sham ($p < 0.05$, Figure 4(a)). Exogenous administration r-LRP1 showed significantly higher protein expression of LRP1 compared to vehicle ($p < 0.05$). LRP1 siRNA given alone and with r-LRP1 displayed decreased expression compared to vehicle ($p < 0.05$) and were not significantly changed compared to sham ($p > 0.05$). Control siRNA did not show any difference when compared to vehicle ($p > 0.05$).

Hx was significantly elevated for all groups compared to the sham group ($p < 0.05$, Figure 4(b)). ICH with the r-LRP1 treatment showed significant elevation of Hx expression when compared to vehicle ($p < 0.05$). However, LRP1 siRNA was able to reverse this effect when given with r-LRP1 on Hx expression and was no longer significant to vehicle ($p > 0.05$). LRP1 siRNA and control siRNA without r-LRP1 did not show any changes compared to vehicle ($p > 0.05$).

Double immunofluorescence staining was completed in the perihematoma brain tissue (Figure 4(c), large dash line circle is perihematoma, small dash line circle is hematoma). Fluorescent staining found that LRP1 was colocalized with microglia (Iba-1), astrocytes (GFAP), and endothelial cells of the brain vessels (vWF; Figure 4(d) to (f)). Additionally, fluorescence of LRP1 revealed increased expression in vehicle, r-LRP1, and control siRNA groups while showing decreased expression in LRP1 siRNA and LRP1 siRNA with r-LRP1 groups, confirming similar Western blot results. Hx was also found to be colocalized with microglia and was increased in all groups compared to sham (Figure 4(g)).

r-LRP1 decreases oxidative stress and neuronal apoptosis after ICH

Compared with vehicle-treated ICH, Western blot analysis found that exogenous r-LRP1 treatments reduced protein expression of MDA, caspase 3, and cleaved caspase 3 and increased SOD1 expression ($p < 0.05$, Figure 5(a) to (f)). r-LRP1 given with LRP1 siRNA results show that these protective effects tended to be reversed and were no longer significant to vehicle for all proteins ($p > 0.05$). LRP1 and control siRNA groups without r-LRP1 did not display any changes compared to vehicle ($p > 0.05$). All groups subjected to ICH displayed significantly different protein expression compared to sham animals ($p < 0.05$).

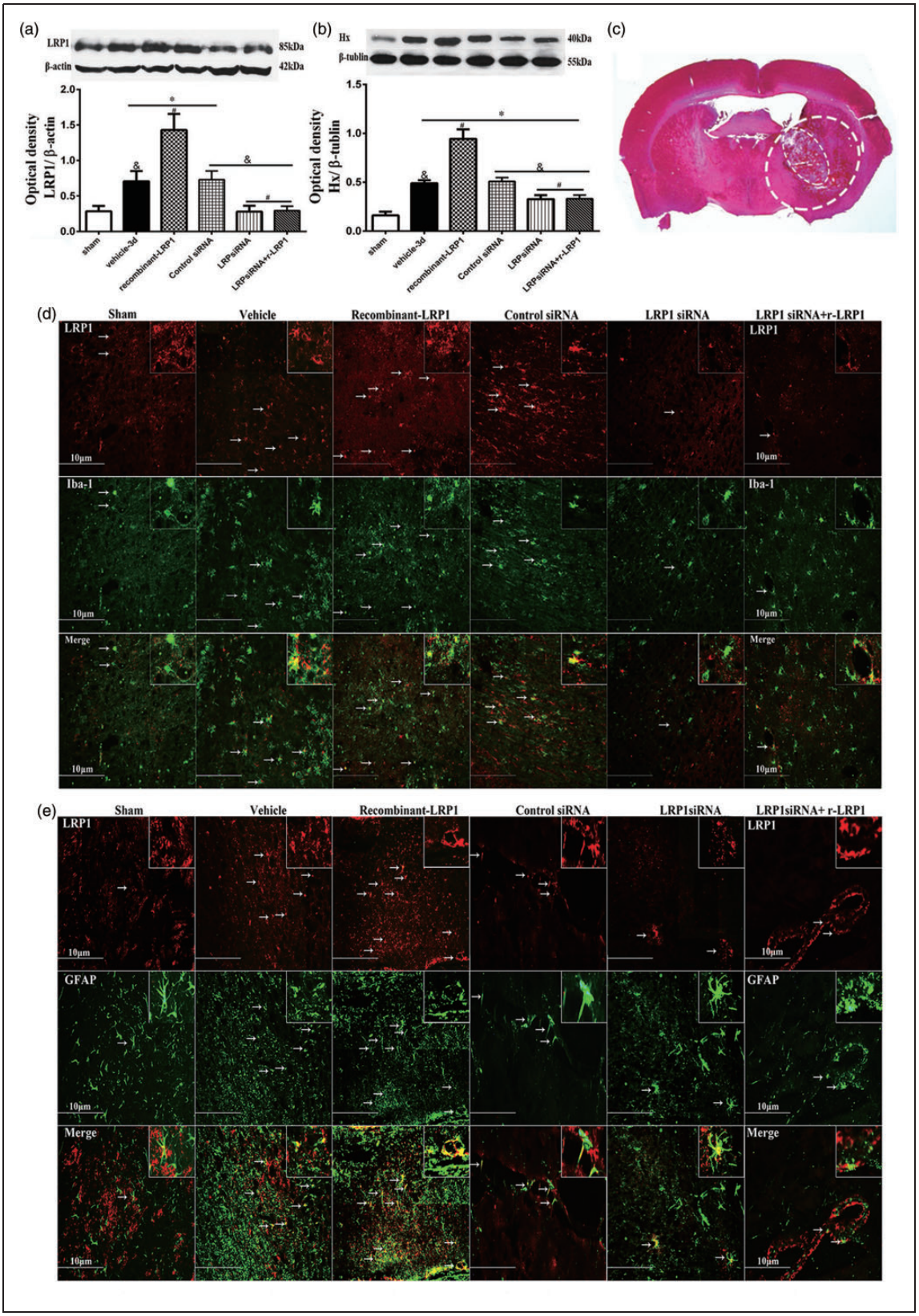

Figure 4. Effect of LRP1 on hemopexin associated with ICH 72 h after surgery. Representative images are shown of Western blot assay for LRP1 and hemopexin (Hx) level within ipsilateral brain tissues (a and b) (n = 5/group). One-way ANOVA followed by Tukey tests were used. *$p < 0.05$ versus sham; #$p < 0.05$ versus vehicle; &$p < 0.05$ versus human recombinant LRP1-treated ICH. Representative immunohistochemistry microphotographs of LRP1 and hemopexin with Iba-1 (d and g), LRP1 and GFAP (e), LRP1 and vWF (f) within perihematoma brain tissues (c) revealed that LRP1 and Hx expression were colocalized with microglia (scale bar: 10 μm).

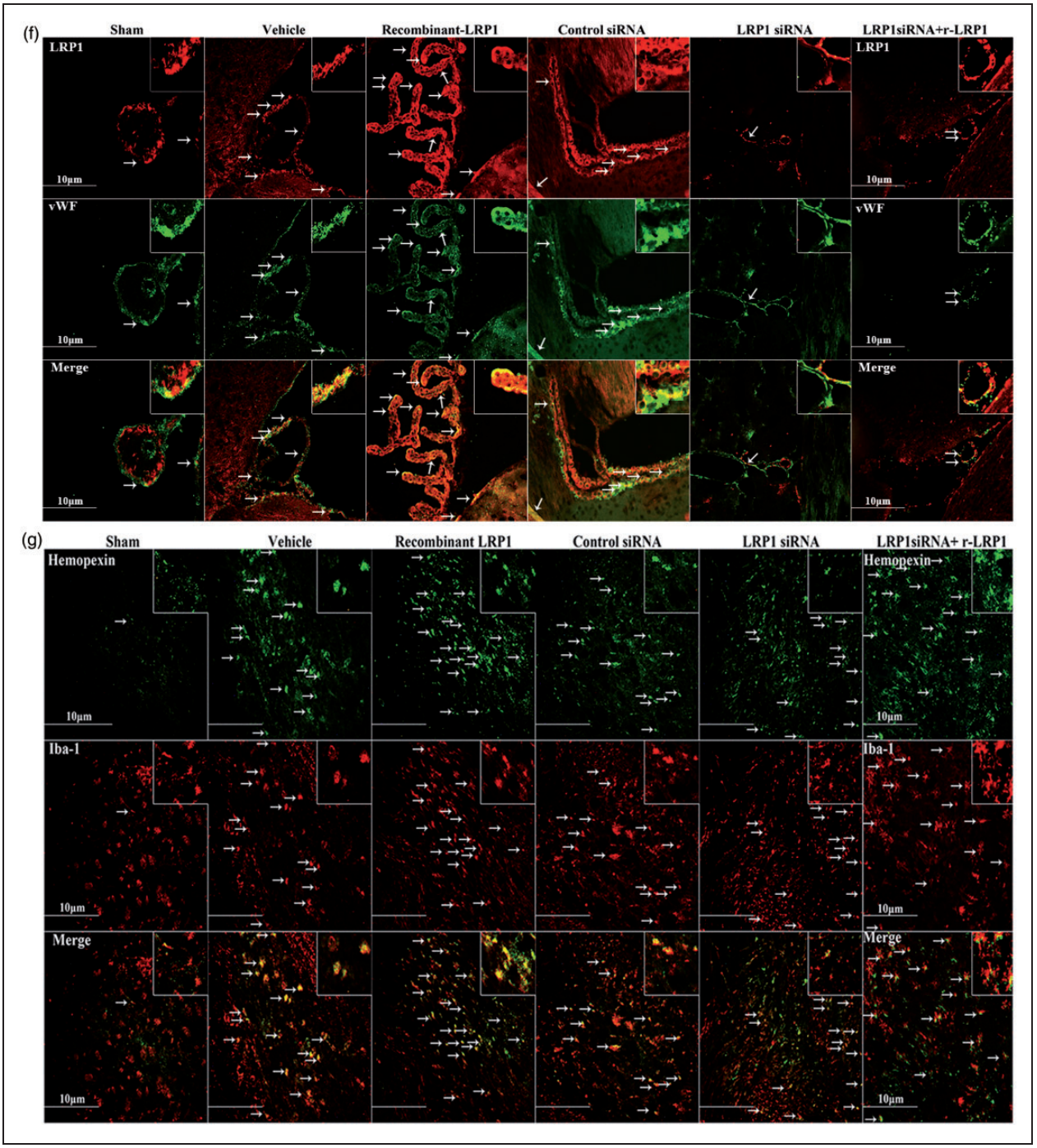

Figure 4. continued.

FJC staining with neuron-specific nuclear antigen (NeuN) was used to determine apoptosis of neurons. It was found that fewer cells displayed FJC in the r-LRP1 treatment group compared to vehicle suggesting a decrease in cell death. Additionally, fewer FJC cells co-stained with NeuN were seen to express FJC in the r-LRP1 group suggesting less neuronal apoptosis. FJC with NeuN staining also reveals elevated neuron apoptosis in LRP1 and control siRNA groups. ICH animals given LRP1 siRNA and r-LRP1 together also display higher apoptosis of neurons compared to the sham group. However, this also shows that r-LRP1 was not able to reverse the effects of LRP1 siRNA to decrease apoptosis.

Double immunofluorescence staining of FJC with NeuN was done and found not only in degenerating

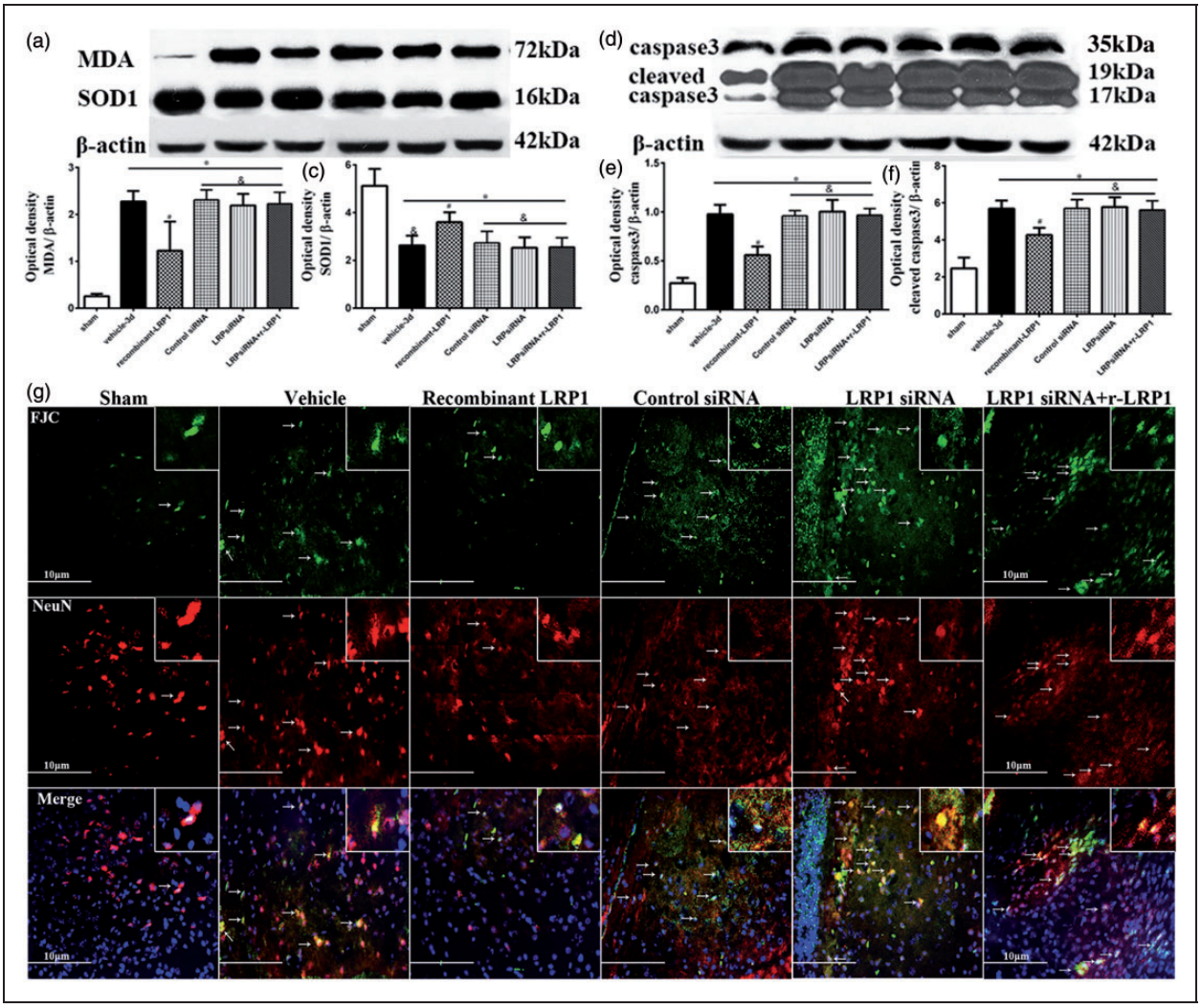

Figure 5. Effect of LRP1 on oxidative stress and neuronal apoptosis associated with ICH 72 h after surgery. Compared with the vehicle-treated ICH, rhLRP1 reduced levels of malondialdehyde (MDA; a and b), caspase 3 (d and e), cleaved caspase 3 (d and f) and elevated SOD1 (a and c) by ICH, the protective effects of which tended to be reversed by siRNA for LRP1 administration ($n = 5$/group). One-way ANOVA followed by Tukey tests were used. *$p < 0.05$ versus sham; #$p < 0.05$ versus vehicle; &$p < 0.05$ versus human recombinant LRP1-treated ICH. FJC staining with immunofluorescence to NeuN was found not only in degenerating nerve cell bodies but also in periventricular or perivascular cell bodies, microglias and blood cells (g). Arrows indicate cells with positive staining. Scale bar: 10 μm.

nerve cell bodies but also in periventricular or perivascular cell bodies, microglias, and blood cells (Figure 5(g)). The images showed the similar trend of above mentioned results by Western blot.

Discussion

In the present study, we have made the following observations: (1) endogenous LRP1 and Hx levels were significantly elevated in ipsilateral brain tissues at 1 day and up to 14 days after surgery in a mouse collagenase ICH model; they reached a peak at days three to seven after ICH. (2) Neurobehavior test scores lowered 6 h, 24 h, and three days after ICH compared with sham mice; hemoglobin levels, brain edema, and BBB permeability elevated three days after ICH; (3) exogenous human recombinant LRP1 protein significantly attenuated hematoma volume, ICH-induced brain edema, BBB permeability and neurological deficits at three days after ICH; (4) siRNA of LRP1 reversed the benefits of recombinant LRP1 on neurological outcomes at three days after ICH; (5) the improved outcomes by exogenous human recombinant LRP1 were associated with enhanced heme scavenging and less oxidative stress (MDA/SOD1) along with brain cells injury (FJC, caspase 3, and cleaved caspase 3 level) in

ipsilateral brain tissues three days after ICH; (6) siRNA for LRP1 partially offset the neuroprotection (heme phagocytosis, oxidative stress, and brain cells injury) provided by recombinant LRP1 3 days after ICH. These results demonstrate that LRP1 is involved in heme scavenging and BBB protection in adjacent hematoma brain tissues after ICH.

A central pathophysiologic event after ICH is the massive release of heme from red blood cells into the extracellular space. Free heme triggers oxidative stress and is highly proinflammatory.[29] It has been demonstrated previously that the concentration of both nonheme iron and iron-handling proteins significantly increased three days after ICH.[30,31] Therefore, the potential beneficial effects of the heme scavenging in the study were evaluated at day 3 after ICH induction.

Following ICH, lysed erythrocytes and hemoglobin degradation products resulted in delayed edema and BBB disruption.[32,33] The amplified processes of injury in ICH may be due to heme-catalyzed oxidative stress and lipid peroxidation then trigger apoptosis after ICH.[34] FJC possesses a highest affinity for the endogenous neurodegeneration molecules,[35] it is a reliable and effective marker of neuronal cell death.[36] Neuronal death after ICH is mediated in part by apoptotic mechanisms.[34] Caspase-dependent mechanisms play a crucial role in the lesion development caused by the blood effect on brain tissue.[37] We found there were higher levels of MDA, caspase 3, cleaved caspase 3, and FJC-labeled neurons accompanied by increased hemoglobin levels, brain water contents, and Evans blue extravasation three days after ICH in the ipsilateral tissues of ICH animal, suggesting that the increased oxidative stress, apoptosis, and neurons death followed with high hematoma volume, cerebral edema, and BBB disruption occurred three days after ICH. Meanwhile, there were a decrease in neurobehavior test scores and SOD1 levels, it suggested an impairment in neurological function and antioxidation.

After hemolysis and the subsequent release of heme from hemoglobin, several pathways are employed to transport and metabolize this heme and its iron moiety to protect the brain from potential oxidative stress.[38] Oxidative stress is thought to be a key reason for delayed injury after ICH, which is likely due to free-Fe catalyzed free radical reactions. Such events include oxidative stress mediated by free Fe that originated from hemoglobin breakdown. Therefore, minimizing the damage caused by oxidative stress following hemoglobin breakdown and Fe release is a major therapeutic target.[39]

The only known Hx:heme receptor is the LRP1, also known as a2 macroglobulin receptor or CD 91, acts as a heme scavenger, a signaling receptor and transports multiple binding partners, including apoE, α-2-macroglobulin, tissue plasminogen activator, plasminogen activator inhibitor-1, factor VIII, lactoferrin, and Aβ, which is the main efflux pump of Aβ from the brain to the blood.[40,43] In humans, LRP1 is a major Aβ clearance receptor in cerebral vascular smooth muscle cell, and a disturbance of this pathway contributes to Aβ accumulation.[42] Deletion of LRP1 significantly alters the integrity of neuronal membranes, dendritic spines, and synapses in adult mice.[44] Meanwhile, deletion of macrophage LRP1 creates an imbalance between efferocytosis and apoptosis susceptibility resulting in enhanced inflammation, lesion cell death, and plaque necrosis.[45] LRP1 is ubiquitously expressed and has a low affinity for the Hx/heme complex. In the present study, there were significant increases in the Hx and LRP1 protein levels at 1 day and up to 14 days after ICH, the results showed that accumulation of heme in ICH triggered its removal-signaling pathway. Meanwhile, we found that LRP1 is expressed in cerebrovasculature, in particular in choroid plexus, perivascular microglias, and foot process of astroglias, which showed that LRP1 took part in transvascular scavenging system through BBB in brain. The results showed that LRP1 (specially expressed in choroid plexus) should play an important role in scavenging heme in this in vivo ICH model. Drug delivered through the CSF compartment could penetrate into the brain parenchyma and circulate into blood along CSF flow tracks.[46]

We hypothesize that due to the massive release of heme following ICH, LRP1 system is completely saturated and is unable to scavenge heme. Similar hypothesis regarding saturation of LRP1 system in human patients after SAH was discussed previously.[22] Accumulation of the free heme accelerates tissue damage by promoting peroxidative reactions and activation of inflammatory cascades.[47] Increasing the capacity of the system via administration of the recombinant LRP1 seemed to be a promising and clinical relevant approach. So we use recombinant LRP1 to enhance LRP1 expression at the BBB.

Intracerebroventricular human recombinant LRP1 administration reduced hematoma volumes, brain edema, BBB permeability as well as oxidative stress, apoptosis, neuron death, and better neurological scores three days after ICH, thus demonstrating a beneficial overall outcome after ICH. Inhibition of LRP1 expression with RAP (a specific LRP1 receptor antagonist) and LRP1 siRNA (LRP1 knockdown) could significantly block LRP1 function and significantly blocked both basal and intravenous immunoglobulin (IVIG)-induced Aβ efflux from inner to outer chambers.[48] In vivo LRP1 knock-out mice demonstrated that Aβ clearance in brain is impaired[49] and a significant neurodegeneration in the hippocampus and cortex in the absence of amyloid pathology.[44] Consistent with this, our study used intracerebroventricular LRP1

siRNA administration and found suppressed LRP1 expression in brain and further reversed the protective effect of exogenous human recombinant LRP1, confirming the protective role of LRP1 in ICH pathological progression.

Taken together, the release of cell-free heme is a major pathological factor after ICH, which leads to the oxidative stress, increased inflammation, apoptosis and consequently to the disruption of BBB, development of brain edema and impairment of neurological functions. Pharmacological manipulations increasing heme–Hx clearance represent a novel, clinical relevant strategy that is able to attenuate the ICH-induced pathophysiology. Our results demonstrated that recombinant LRP1 administration resulted in the raise of LPR1 positive cell number, which is a sign of the activation of heme–Hx clearance system. The activation of the heme–Hx system resulted in SOD1 upregulation and subsequently in the decrease of oxidative stress as well as attenuation of post-ICH apoptosis. This beneficial effects of LRP1 administration improved BBB integrity, resulted in the attenuation of brain edema formation and in the improvement of neurological functions.

In conclusion, signaling through LRP1 appears to be a common platform controlling heme scavenging after ICH. Our study underscores the role of LRP1 achieved by local administration of human recombinant LRP1 in the setting of ICH. Selective LRP1 blockade partially reversed the neuroprotective effects associated with LRP1 supplement. LRP1 may offer pleiotropic protective effects through promoting heme resolution and diminishing brain edema after ICH and may thus prove beneficial to post-ICH outcomes.

Funding

This study was supported by NIH P01 NS082184-01 to JHZ.

Declaration of conflicting interests

The author(s) declared no potential conflicts of interest with respect to the research, authorship, and/or publication of this article.

Authors' contributions

GW conducted the experiments, analyzed data and drafted the manuscript. AM worked on the research design, experiments and manuscript preparation. AS, YO, PY and EB participated in the conduction of the experiments. DN helped in neurobehavioral tests and manuscript preparation. JHZ and JT worked on research design, data analysis and interpretation, and manuscript preparation.

References

1. Schlunk F and Greenberg SM. The pathophysiology of intracerebral hemorrhage formation and expansion. *Transl Stroke Res* 2015; 6: 257–263.
2. Chen S, Yang Q, Chen G, et al. An update on inflammation in the acute phase of intracerebral hemorrhage. *Transl Stroke Res* 2015; 6: 4–8.
3. Aronowski J and Zhao X. Molecular pathophysiology of cerebral hemorrhage: Secondary brain injury. *Stroke* 2011; 42: 1781–1786.
4. Baechli H, Behzad M, Schreckenberger M, et al. Blood constituents trigger brain swelling, tissue death, and reduction of glucose metabolism early after acute subdural hematoma in rats. *J Cereb Blood Flow Metab* 2010; 30: 576–585.
5. Wagner KR, Sharp FR, Ardizzone TD, et al. Heme and iron metabolism: Role in cerebral hemorrhage. *J Cereb Blood Flow Metab* 2003; 23: 629–652.
6. Xi G, Keep RF and Hoff JT. Mechanisms of brain injury after intracerebral haemorrhage. *Lancet* 2006; 5: 53–63.
7. Wang J and Dore S. Inflammation after intracerebral hemorrhage. *J Cereb Blood Flow Metab* 2007; 27: 894–908.
8. Wang G. The pathogenesis of edema and secondary insults after ICH. In: Chaudhary V (ed) *Intracerebral hemorrhage*. Rijeka, Croatia: IN TECH, 2014, pp. 25–40.
9. Xiong XY, Wang J, Qian ZM, et al. Iron and intracerebral hemorrhage: from mechanism to translation. *Transl Stroke Res* 2014; 5: 429–441.
10. Zhao X and Aronowski J. Nrf2 to pre-condition the brain against injury caused by products of hemolysis after ich. *Transl Stroke Res* 2013; 4: 71–75.
11. Zlokovic BV. Neurodegeneration and the neurovascular unit. *Nat Med* 2010; 16: 1370–1371.
12. Sagare AP, Deane R and Zlokovic BV. Low-density lipoprotein receptor-related protein 1: a physiological abeta homeostatic mechanism with multiple therapeutic opportunities. *Pharmacol Ther* 2012; 136: 94–105.
13. Ramanathan A, Nelson AR, Sagare AP, et al. Impaired vascular-mediated clearance of brain amyloid beta in Alzheimer's disease: the role, regulation and restoration of lrp1. *Front Aging Neurosci* 2015; 7: 136.
14. Lillis AP, Van Duyn LB, Murphy-Ullrich JE, et al. Ldl receptor-related protein 1: unique tissue-specific functions revealed by selective gene knockout studies. *Physiol Rev* 2008; 88: 887–918.
15. Ramanathan A, Nelson AR, Sagare AP, et al. Impaired vascular-mediated clearance of brain amyloid beta in Alzheimer's disease: the role, regulation and restoration of lrp1. *Front Aging Neurosci* 2015; 7: 136.
16. Nielsen MJ, Moller HJ and Moestrup SK. Hemoglobin and heme scavenger receptors. *Front Aging Neurosci* 2010; 12: 261–273.
17. Hvidberg V, Maniecki MB, Jacobsen C, et al. Identification of the receptor scavenging hemopexin-heme complexes. *Blood* 2005; 106: 2572–2579.
18. Kumar S and Bandyopadhyay U. Free heme toxicity and its detoxification systems in human. *Toxicol Lett* 2005; 157: 175–188.
19. Piccard H, Van den Steen PE and Opdenakker G. Hemopexin domains as multifunctional liganding modules in matrix metalloproteinases and other proteins. *J Leukoc Biol* 2007; 81: 870–892.

20. Xu H, Perreau VM, Dent KA, et al. Iron regulates apolipoprotein e expression and secretion in neurons and astrocytes. *J Alzheimers Dis* 2016; 51: 471–487.
21. Cao C, Pressman EK, Cooper EM, et al. Placental heme receptor lrp1 correlates with the heme exporter flvcr1 and neonatal iron status. *Reproduction* 2014; 148: 295–302.
22. Garland P, Durnford AJ, Okemefuna AI, et al. Heme-hemopexin scavenging is active in the brain and associates with outcome after subarachnoid hemorrhage. *Stroke* 2016; 47: 872–876.
23. Wu B, Ma Q, Suzuki H, et al. Recombinant osteopontin attenuates brain injury after intracerebral hemorrhage in mice. *Neurocrit Care* 2011; 14: 109–117.
24. Manaenko A, Lekic T, Ma Q, et al. Hydrogen inhalation ameliorated mast cell-mediated brain injury after intracerebral hemorrhage in mice. *Crit Care Med* 2013; 41: 1266–1275.
25. Manaenko A, Fathali N, Chen H, et al. Heat shock protein 70 upregulation by geldanamycin reduces brain injury in a mouse model of intracerebral hemorrhage. *Neurochem Int* 2010; 57: 844–850.
26. Manaenko A, Chen H, Kammer J, et al. Comparison evans blue injection routes: intravenous versus intraperitoneal, for measurement of blood-brain barrier in a mice hemorrhage model. *J Neurosci Methods* 2011; 195: 206–210.
27. Huang L, Sherchan P, Wang Y, et al. Phosphoinositide 3-kinase gamma contributes to neuroinflammation in a rat model of surgical brain injury. *J Neurosci* 2015; 35: 10390–10401.
28. Guo H, Liu J, Van Shura K, et al. N-acetyl-aspartyl-glutamate and inhibition of glutamate carboxypeptidases protects against soman-induced neuropathology. *NeuroToxicology* 2015; 48: 180–191.
29. Hu X, Tao C, Gan Q, et al. Oxidative stress in intracerebral hemorrhage: sources, mechanisms, and therapeutic targets. *Oxid Med Cell Longev* 2016; 2016: 3215391.
30. Wu J, Hua Y, Keep RF, et al. Iron and iron-handling proteins in the brain after intracerebral hemorrhage. *Stroke* 2003; 34: 2964–2969.
31. Nakamura T, Keep RF, Hua Y, et al. Deferoxamine-induced attenuation of brain edema and neurological deficits in a rat model of intracerebral hemorrhage. *J Neurosurg* 2004; 100: 672–678.
32. Qing WG, Dong YQ, Ping TQ, et al. Brain edema after intracerebral hemorrhage in rats: the role of iron overload and aquaporin 4. *J Neurosurg* 2009; 110: 462–468.
33. Huang FP, Xi G, Keep RF, et al. Brain edema after experimental intracerebral hemorrhage: Role of hemoglobin degradation products. *J Neurosurg* 2002; 96: 287–293.
34. Matsushita K, Meng W, Wang X, et al. Evidence for apoptosis after intercerebral hemorrhage in rat striatum. *J Cereb Blood Flow Metab* 2000; 20: 396–404.
35. Xuan W, Vatansever F, Huang L, et al. Transcranial low-level laser therapy improves neurological performance in traumatic brain injury in mice: effect of treatment repetition regimen. *PLoS One* 2013; 8: e53454.
36. Chidlow G, Wood JP, Sarvestani G, et al. Evaluation of fluoro-jade C as a marker of degenerating neurons in the rat retina and optic nerve. *Exp Eye Res* 2009; 88: 426–437.
37. Alessandri B, Nishioka T, Heimann A, et al. Caspase-dependent cell death involved in brain damage after acute subdural hematoma in rats. *Brain Res* 2006; 1111: 196–202.
38. Wagner KR, Sharp FR, Ardizzone TD, et al. Heme and iron metabolism[colon] role in cerebral hemorrhage. *J Cereb Blood Flow Metab* 2003; 23: 629–652.
39. Hackett MJ, DeSouza M, Caine S, et al. A new method to image heme-fe, total fe, and aggregated protein levels after intracerebral hemorrhage. *ACS Chem Neurosci* 2015; 6: 761–770.
40. Lin L and Hu K. Lrp-1: functions, signaling and implications in kidney and other diseases. *Int J Mol Sci* 2014; 15: 22887–22901.
41. Sagare A, Deane R, Bell RD, et al. Clearance of amyloid-beta by circulating lipoprotein receptors. *Nat Med* 2007; 13: 1029–1031.
42. Kanekiyo T, Liu CC, Shinohara M, et al. Lrp1 in brain vascular smooth muscle cells mediates local clearance of alzheimer's amyloid-beta. *J Neurosci* 2012; 32: 16458–16465.
43. Storck SE, Meister S, Nahrath J, et al. Endothelial lrp1 transports amyloid-beta1-42 across the blood-brain barrier. *J Clin Invest* 2016; 126: 123–136.
44. Liu Q, Trotter J, Zhang J, et al. Neuronal lrp1 knockout in adult mice leads to impaired brain lipid metabolism and progressive, age-dependent synapse loss and neurodegeneration. *J Neurosci* 2010; 30: 17068–17078.
45. Yancey PG, Blakemore J, Ding L, et al. Macrophage lrp-1 controls plaque cellularity by regulating efferocytosis and akt activation. *Arterioscler Thromb Vasc Biol* 2010; 30: 787–795.
46. Kuo A and Smith MT. Theoretical and practical applications of the intracerebroventricular route for CSF sampling and drug administration in CNS drug discovery research: a mini review. *J Neurosci Methods* 2014; 233: 166–171.
47. Belcher JD, Beckman JD, Balla G, et al. Heme degradation and vascular injury. *Antioxid Redox Signal* 2010; 12: 233–248.
48. Gu H, Zhong Z, Jiang W, et al. The role of choroid plexus in IVIG-induced beta-amyloid clearance. *Neuroscience* 2014; 270: 168–176.
49. Kanekiyo T, Cirrito JR, Liu CC, et al. Neuronal clearance of amyloid-beta by endocytic receptor lrp1. *J Neurosci* 2013; 33: 19276–19283.